Pyrazinoic acid-Poly(malic acid) biodegradable nanoconjugate for efficient intracellular delivery

Simone Pinto Carneiro[a,b], Laurence Moine[a], Barbara Tessier[a], Valérie Nicolas[a], Orlando David Henrique dos Santos[b], Elias Fattal[a∗]

[a]Institut Galien Paris-Sud, CNRS, Université Paris-Sud, Université Paris-Saclay, 92296 Châtenay-Malabry, France
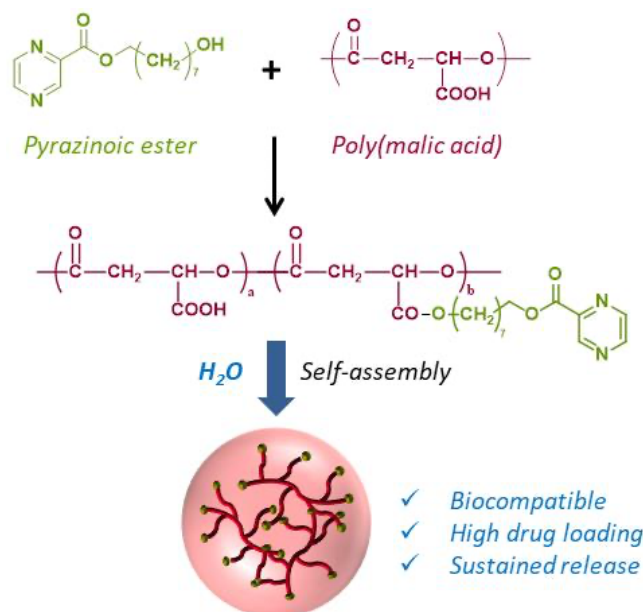
[b]Laboratório de Fitotecnologia, Escola de Farmácia, Universidade Federal de Ouro Preto, 35400000, Ouro Preto, Brazil

Graphical abstract:

Abstract

Tuberculosis is an infectious disease affecting mostly lungs, that is still considered a health global problem as it causes millions of deaths worldwide. Current treatment is effective but associated with severe adverse effects due to the high doses of each anti-tuberculosis drug daily administrated by oral therapy. For the first time, a pyrazinoic acid (PA) biodegradable nanoconjugate was synthesized and developed for pulmonary administration in an attempt to reduce the administered doses by achieving a high drug payload and controlled release at the target site. The conjugate was synthesized by coupling pyrazinoic acid on carboxylic groups of poly(malic acid), which is a biodegradable and biocompatible polymer, and posteriorly self-assembled into nanoconjugates. Characterization confirmed the formation of nanometric, spherical and negatively charged pyrazinoic acid nanoconjugate (NC-PA). NC-PA was stable for 60 days at 4 and 37°C and able to deliver PA in a sustained release manner over time. On macrophages, they exhibited no cell toxicity for a wide range of concentrations (from 1 to 100 µg/mL), demonstrating the safety of NC-PA. In addition, the nanoconjugate was efficiently taken up by RAW 264.7 cells over 6 hours reaching a maximum value after 3 hours of incubation. In conclusion, innovative nanoconjugates are a promising alternative to deliver drugs directly to the lungs and contributing to improving tuberculosis therapy.

∗ Corresponding author: Université Paris-Sud, Faculté de Pharmacie, Institut Galien Paris-Sud, UMR CNRS 8612, 5 rue JB Clément, 92296 Châtenay-Malabry, Cedex, France. Email: elias.fattal@u-psud.fr

Abbreviations

pyrazinoic acid (PA)
poly(malic acid) PMA
pyrazinoic acid nanoconjugate (NC-PA)
pyrazinamide (PZA)

Rationale and purpose

Tuberculosis (TB) treatment remains a significant clinical challenge. It is still necessary to improve bioavailability and reduce the administration frequency of anti-tuberculosis drugs. A promising approach consists to develop a nanomedicine out of a poly (malic acid) conjugate with a high drug loading rate and a controlled release process avoiding commonly observed drug leakage. The process was applied to an anti-tuberculosis drug: pyrazinoic acid providing low toxicity and high intracellular penetration in order to target intracellular bacteria.

Introduction

Tuberculosis (TB) is an infectious disease caused by *Mycobacterium tuberculosis*, a pathogen that resides partially within alveolar macrophages.[1] TB is considered worldwide as one of the leading causes of death produced by a single infectious agent. It is regarded by many countries as public health and social concerns.[2] The World Health Organization recommends a treatment guideline that comprises the association of 4 anti-tuberculosis drugs within a minimum six-month period.[2] However, daily high doses of each drug required for an effective patient response are associated with the occurrence of systemic and severe adverse effects, mostly hepatotoxicity, affecting consequently patient compliance.[3],[4] Failed therapy contributes to the emergence of bacteria multidrug-resistant TB that additionally demands the introduction of second-line anti-tuberculosis drugs into the therapeutic regimen, elongating the period of treatment and culminating in much more toxic side-effects.[5]

Pyrazinamide (PZA) is one of the 4 first-line anti-tuberculosis drugs used in the standard protocol of TB treatment. Since PZA was introduced, TB therapy was shortened from 12 to 6 months due to its specific ability to act against non-growing tubercle bacilli resident inside the acidic pH of phagosome that cannot be killed by other anti-tuberculosis drugs.[6],[7] When combined with rifampicin or isoniazid, PZA exhibits unique sterilizing and synergistic effects making this drug essential for a successful treatment. The PZA mechanism of action is still unknown; however, Zhang and co-workers[6] produced the hypothesis that PZA is a prodrug that enters the bacilli and is converted into its active moiety, the pyrazinoic acid (PA), through the action of the mycobacterial enzyme pyrazinamidase. Although PA is known as the active PZA metabolite, the use of this drug alone is not recommended, because of its poor lipophilicity and high-ionized state at physiological pH that limit its diffusion and passage through the bacilli cell wall, leading to the drug low bioavailability.[8],[9] Recently, the synthesis of alternative PA prodrugs which do not require bioactivation by an enzyme arose as a smart strategy for overcoming the above limitations. Cynamon et al.[10] have proposed novel PA esters with better anti-mycobacterial activity than PZA itself; the same encouraging result with the additional finding of improved drug stability in serum was demonstrated by Simões et al.[11] after evaluating conjugates of PA esters and amide derivatives, reinforcing the potential of these ester products to be more effective than PZA against mycobacteria.

Direct administration of anti-tuberculosis drugs to the lungs offers major advantages over traditional oral therapy.[12]–[14] First, the pulmonary route allows the delivery of drugs directly on the TB target site – the alveolar macrophages. Then, local delivery can achieve a high drug concentration at the site of infection with the intention of improving therapeutic effect and reducing

systemic exposure. Sung et al.[15] corroborated this hypothesis by developing a dry powder composed of rifampicin porous nanoparticle-aggregate particle and performing a pharmacokinetic study in vivo. Formulations administered by intratracheal insufflation were effective in maintaining rifampicin amounts in the lungs over a longer period of 8 hours, whereas after oral or intravenous delivery, no more rifampicin was detected. Interestingly, the same pulmonary route was tested for the administration of an aerosol without the nanoparticle formulation and rifampicin was not detected in the lungs after 8 hours, emphasizing the advantageous strategy of delivering nanoparticles via the pulmonary route.

Numerous studies on the design of nanoparticle-based anti-TB drugs over the past decade report their potential to improve drug bioavailability and reduce drug dosing frequency.[14],[16]–[18] However, despite promising results, physical loading of anti-TB drugs in nanoparticles was characterized by a poor loading efficiency and a burst release. As an alternative strategy, in this work, drug-polymer conjugation has been considered to improve the absorption and bioavailability of anti-TB-type medications. Compared to conventional nanoparticles, nanoconjugates reveal attractive properties including high-loading capacity and sustained release without drug leakage.[19],[20] After administration, these nanoconjugates can be easily degraded through an enzymatic or hydrolytic mechanism, releasing the active molecule directly on the target site.

In the field of drug delivery systems, several (bio)degradable polymers have been studied to formulate polymer-drug conjugates. Among them, poly(malic acid) (PMA), an aliphatic polyester, has been proven to be a promising candidate.[21] In addition to these excellent degradation and biocompatibility properties, the presence of a carboxyl group on each repeating unit allows for chemical modification with a large spectrum of therapeutic molecules. It has been extensively investigated as a water-soluble, biodegradable, and biocompatible polymer with remarkable advantages in clinical use.[22]

The nanoconjugate, we designed, is based on poly(malic acid), a water-soluble polyester. PA was chemically conjugated to the polyester backbone via a hydrolysable carboxylic acid ester linker. To improve the stability and afford self-assembly of the conjugate system, a hydrophobic spacer was introduced between the polymer and the drug. After synthesis, the self-assembly behavior was studied and characterized, and in vitro release was investigated. Cytotoxicity and nanoconjugate cell uptake were evaluated on macrophages, the cell target.

Materials and Methods

For synthesis experiments, all solvents were of analytical or high-performance liquid chromatography-grade. L-malic acid, N,N – dicyclohexylcarbodiimide (DCC) and 4-dimethyl aminopyridine (DMAP) were purchased from Sigma-Aldrich (France). PA and 1,8-octanediol were provided by TCI (Europe, N.V.). Rhodamine B-PLGA was supplied from PolySciTech (USA). All reagents were used as received. For cell culture experiments, Dulbecco's Modified Eagle Medium (DMEM), 3-[4,5-dimethylthiazol-2-yl]-3,5 diphenyl tetrazolium bromide (MTT), penicillin, streptomycin, and phosphate buffered saline (PBS) were purchased from Sigma-Aldrich (France). Fetal bovine serum (FBS) was obtained from Thermo Fischer Scientific (USA).

Experimental

Synthesis of PMA

PMA was obtained by polycondensation of L-malic acid.[23] 5 g of L-malic acid (37 mmol) was added into a Schlenk flask and heated at 110 ºC during 72h under 0.7-1 mmHg. The viscous product was dissolved in tetrahydrofuran (THF) and purified twice by precipitation into a diethyl ether:petroleum ether (60:40). The precipitated polymer was dissolved in purified water and freeze-dried for 24 hours (Alpha 2-4 LD Plus, Christ). L-malic conversion = 76% (^{1}H NMR).

Synthesis of PA conjugates

PA conjugate was obtained by esterification reactions, performed in 2 steps.

Step 1: Synthesis of intermediate PA:Oct product. 2 g of PA (16.1 mmol) and 2.3 g of

1,8-octanediol (16.1 mmol) were dissolved in 80 mL of anhydrous THF. In another round bottom flask, 2.5 g of DCC (12.1 mmol) and 0.2 g of DMAP (1.6 mmol) were dissolved in 40 mL of anhydrous THF. After complete dissolution, DCC:DMAP solution was added dropwise into the PA:1,8-octanediol solution and the reaction went over overnight at room temperature. The reaction mixture was filtered, and the solvent was evaporated. The crude product was purified by column chromatography, using ethyl acetate as eluent. Yield = 50%.

Step 2: Synthesis of PA conjugate. In a round bottom flask, 614 mg of PMA and 466 mg of PA:Oct (molar ratio: $n_{MA\ unit} = 2.9\ n_{PA:Oct}$) were added and dissolved in 20 mL of anhydrous THF. In another flask, 572 mg of DCC (2.78 mmol) and 64.5 mg of DMAP (0.53 mmol) were dissolved in 20 mL of anhydrous THF. Both solutions were maintained under argon flow and magnetic stirring. After complete dissolution, the DCC:DMAP solution was added dropwise to the PMA:Oct solution, at 0°C for 30 minutes. The reaction was carried overnight at room temperature, then filtered and the product was condensed by solvent evaporation. The crude product was dissolved in chloroform and purified twice by precipitation into a diethyl ether:petroleum ether solution (60:40). PA conjugate was dried under vacuum and recovered as a slightly brown powder.

Preparation of PA nanoconjugate

The labeled NC-PA was obtained by the nanoprecipitation method, which is based on nanoparticle formation through rapid diffusion of the solvent into the aqueous phase.[24] Briefly, 5 mg of PA conjugate was dissolved in 0.5 mL of THF. This organic phase was placed into a syringe-pump apparatus and then slowly added to an aqueous phase, composed of 5 mL of purified water, at a constant rate of 7 mL/min and under moderate magnetic stirring. The solvent was evaporated, yielding nanoparticles at 1.0 mg/mL. In addition, fluorescent nanoparticles labeled with Rhodamine B-PLGA were also prepared following the same procedure and replacing the total amount of conjugate to a mixture of 5% of Rhodamine B-PLGA and 95% (w/w) of PA conjugate, labeled NC-PAFLU.

PMA and conjugate characterization

^{1}H NMR spectroscopy was performed in 5 mm tubes in CDCl$_3$ on a Bruker Avance-300 (300 MHz) spectrometer. Intermediate product from PA conjugate synthesis (PA:Oct) was characterized by electrospray ionization mass spectrometry (LTQ- Velos Pro Thermofisher Scientific).

The molar mass and dispersity of polymers were measured by size-exclusion chromatography. Measurements were performed at 30°C with 2 columns from Malvern Panalytical (Viscotek LT4000L Mixed, Low 300 × 8 mm), a triple detection system (Viscotek 270 Dual Detector and Waters 2414 Refractive Index Detector) coupled with a Waters 515 HPLC pump and Waters 717plus Autosampler. THF was used as the eluent with a flow rate of 1 mL/min.

Nanoconjugate characterization

Particle size and zeta potential analysis

NC-PA was characterized by means of particle size and polydispersity index (PDI) through dynamic light scattering technique and zeta potential by electrophoretic mobility. For size distribution measurements, each sample was diluted in purified water (1:10 ratio), while for surface charge measurements, the same dilution ratio was performed in a 1 mM NaCl solution. Analyses were carried out in triplicate on 3 different batches at 20°C, using a Zetasizer Nano Zs (Malvern Instruments, UK).

Transmission electron microscopy (TEM)

Morphology of NC-PA was analyzed by TEM images. 5 µL of nanoconjugate was deposited onto copper grids covered with a formvar film (400 mesh) for 2 minutes. Then, NC-PA were covered with 5 µL of a 0.5% (w/v) uranyl acetate solution, for 30 seconds. Colorant excess was removed with a filter paper and samples were observed in a JEOL JEM-1400 microscope operating at 80 kV with a filament current of about 55 µA, a post-column high-resolution (11 megapixels) and a high-speed camera (SC1000 Orius; Gatan). Data were acquired from Digital Micrograph (Gatan).

Stability tests

NC-PA was stored at refrigerated (4°C) and physiological (37 ± 2°C) conditions for 60 days. Periodically, a sample was collected and

evaluated as particle size and PDI. Analyses were done in triplicate on 3 different batches at 20°C.

In vitro drug release

2 ml of NC-PA at 1.0 mg/ml were separately dispersed into 8 mL of PBS (pH 7.4). Then, aliquots of 0.5 mL were stored into vials, incubated at 37°C under shaking and protected from light. During a period of 5 days, every 12 hours, a sample was collected and frozen. At the end of the experience, samples were unfrozen, and the amounts of PA released at each time point were quantified by an HPLC method described below. Free PA solutions were also prepared in the same conditions and analyzed using the same procedure to follow the potential degradation of the drug.

HPLC system

HPLC was employed to quantify PA amounts. The system was composed of a Waters 1525 Binary HPLC Pump, an injector Waters 2707 Autosampler and an UV-visible Waters 2998 Photodiode Array Detector. Data acquisition was done using the Empower software. PA was assessed following the protocol described by Simões et al.[11] An RP18 Hydro (250 mm × 4.6 mm × 5.0 µm, Phenomenex) column was used at a temperature of 35°C. The eluent was composed of a mixture of acetonitrile and 25 mM phosphate buffer (pH 2.0 adjusted with phosphoric acid) in a proportion of 5:95% (v/v). The isocratic flow rate was 1.0 mL/min and UV detection were set at $\lambda = 267$ nm. PA retention time was 5.47 minutes. Values reported on each time point analysis were plotted on a PA calibration curve (5 – 200 µg/mL) and quantified following the equation $y = 65936x - 92640$ ($R^2 = 0.9999$).

Cell culture assays

Cell culture

Murine alveolar macrophages – RAW 264.7 cells (ATCC® TIB-71™) were cultured in DMEM supplemented with 10% FBS, 50 U/mL penicillin and 50 U/mL streptomycin. Cells were incubated at 37°C in a 5% CO_2 humidified atmosphere and passaged twice a week at a 1:10 ratio.

Cytotoxicity

Cytotoxicity of nanoconjugate was evaluated using the MTT test, as previously described by Mosmann.[25] Cells were seeded at a density of 4000 cells per well in 96-well plates and pre-incubated for 24 hours. Culture medium was discarded, and cells were treated with a different range of nanoconjugate concentration diluted in fresh medium. PA conjugate and pure PA were incubated at 1, 5, 10, 25, 50, and 100 µg/mL with cell culture. Untreated cells were used as control. Plates were incubated for 48 hours and then 20 µL of a 5 mg/mL MTT solution was added in each well for more 2 hours to enable crystals formation. Culture medium was removed and 200 µL of dimethyl sulfoxide was added to dissolve formazan crystals. Plates were shaken for 10 minutes at room temperature (20 ± 2°C) and the absorbance was measured at 540 nm in a microplate reader. Cell viability, expressed as a percentage, was calculated as the absorbance ratio of treated cells to untreated cells (control). The IC_{50}, expressed as the concentration required by each treatment to induce cell death of 50%, was calculated using a sigmoidal regression and Graph-Pad Prism 6 software (USA).

Nanoconjugate cellular uptake

The kinetics of nanoconjugate internalization by RAW 264.7 macrophages was investigated by confocal microscopy, following an adapted protocol described by Grabowski et al.[26] Briefly, cells were seeded at a density of 80000 cells per well in 6-well plates, containing a glass coverslip in each well. 24 hours after incubation at 37°C in a 5% CO_2 humidified atmosphere, non-adherent cells were washed off and all other cells were treated with fluorescent-labeled PA nanoconjugate (NC-PAFLU) at 10 µg/mL diluted in a fresh culture medium. Untreated macrophages were used as control. Cells were re-incubated at the same conditions and, at pre-determined intervals (0.5, 1.5, 3, and 6 hours), they were assessed with an LSM 510 (Zeiss-Meta) confocal microscope equipped with argon (488 nm, 300 mW) and Helium-Neon (543 nm, 5 mW) lasers, and a plan-apochromat 63× objective. Data were acquired from LSM 510 software, version 3.2. In addition, for each pre-determined time evaluated on a microscope, an average of 20 cells was selected and fluorescence was quantified inside them, using ImageJ software.

Statistical analysis

Statistical analysis data are presented as mean values with standard deviation. Statistical analysis was performed with the Prism Graph-Pad 7.0 software and the significance was calculated using a one-way ANOVA method, in which $p < 0.05$ was considered statistically significant (*$p < 0.05$, **$p < 0.005$, *** $p < 0.0005$, **** $p < 0.0001$).

Results and Discussion

Conjugate synthesis and characterization

In this study, it was important to make a judicious choice of the degradable polymer backbone to allow the self-assembly and loading capacity of nanoconjugates. Poly(malic acid) (PMA) has been extensively investigated as a water-soluble, biodegradable, and biocompatible polymer with remarkable advantages in clinical use.[22] PMA is a non-toxic polymer since it degrades into malic acid after administration, which is an intermediate product of carbohydrates metabolism and therefore, non-toxic to cells.[27] In addition, PMA contains multiple carboxylic functions that can be used to introduce molecules of interest via ester hydrolysable linkages affording high payload nanoconjugates.

The copolymer of malic acid carrying PA was synthesized via a simple coupling of the drug on the polymer backbone through an ester cleavable bond, enabling degradation of PMA-conjugate into biocompatible metabolites.

PMA was first prepared by direct polycondensation of L-malic acid which was carried out under reduced pressure without the use of any catalyst.[27] After purification, a high yield was achieved, up to 80%, demonstrating that conditions set for this reaction were suitable to obtain large batches. Formation of PMA was confirmed by ^{1}H NMR analysis through the presence of CH_2 at 2.9 ppm and CH at 5.4 ppm.[28],[29] The molecular weight of the polymer was in the range of 2,000 – 4,000 g/mol.

Then, PA conjugate was synthesized following a 2 steps process. Prior to PA conjugation onto PMA, a hydrophobic spacer was coupled to the drug through its carboxylic function. The use of PA ester instead of PA provides 2 additional ester groups that can be further hydrolyzed to release the drug from the conjugate. Moreover, in a recent study, PA ester analogs have shown a higher efficacy than pyrazinamide.[11] 1,8-Octanediol was coupled to PA through a classical esterification reaction as shown in **Figure 1**. Formation of n-octyl pyrazinoic acid (PA:Oct) was confirmed by mass spectrometry through *m/z* fragment at 252.2 and ^{1}H NMR by the appearance of the signal at 4.4 ppm attributed to COO-CH_2-protons (**Figure S1,** supporting information).
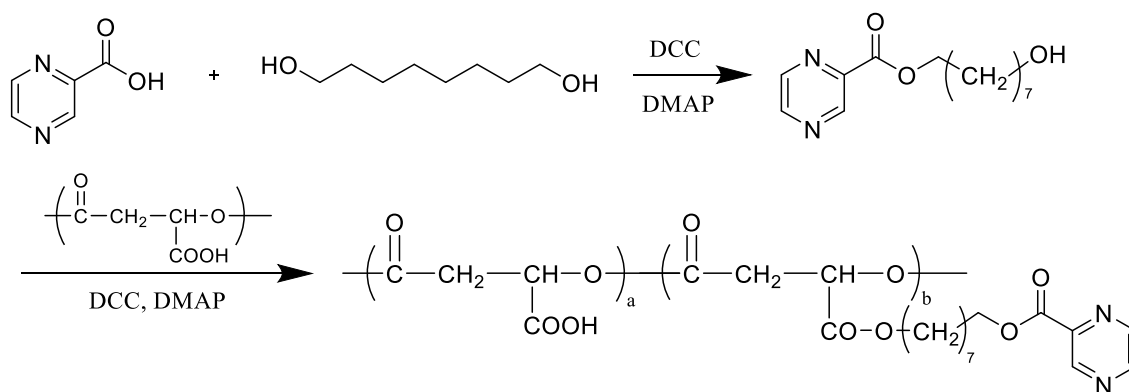

Figure 1. *Synthesis route for pyrazinoic acid ester conjugate (PMA:OctPA).*

The final PA conjugate was obtained as a product of the reaction between PA:Oct and PMA using an initial molar feed ratio OH:COOH of 1:3 **(Figure 1)**. Conjugation was confirmed by ^{1}H NMR with the disappearance of the signal at 3.6 ppm corresponding to the CH_2 in α of hydroxyl group and appearance of a signal at 4.15 ppm attributed to PMA-COO-CH_2- protons (**Figure S2,** supporting information). Additional two-dimensional correlation (COSY) NMR spectroscopy experiments corroborated the appearance of the CH_2 in α of the ester bond to the PMA polymeric chain proving the success of the

conjugation. Analysis of the ^{1}H NMR spectrum indicates $20 \pm 5\%$ of PA:Oct residues coupled to PMA which is satisfactory according to the initial feed. This feed composition corresponds to approximately 30 wt% pyrazinoic ester residues (~ 16 wt% PA).

Nanoconjugate formation

Nanoconjugates were prepared by a simple process of nanoprecipitation taking advantage of the amphiphilic character of PA conjugate which easily self-assembled into nanoparticles in aqueous solution. This method is very accurate to produce monodisperse and stable nanoparticles, without the addition of surfactant and without the use of toxic solvents.[30] Dynamic light scattering analyses showed uniform distributions of size with an average diameter around 145 nm and a low PDI of 0.13. Mean zeta potential evidenced a negatively surface charge of −58 mV, consistent with the presence of non-conjugated carboxylic residues on the final product which considerably influences the surface charge of the resulting nanoconjugate.

To visualize their morphology and size, nanoconjugates were imaged by TEM with negative staining. As shown in **Figure 2**, a rather homogenous particle size population was observed with an average diameter between 150 and 200 nm, which was consistent with DLS data. Moreover, TEM results also evidenced the spherical shape of nanoconjugates and the absence of particle aggregation even without the use of stabilizers.
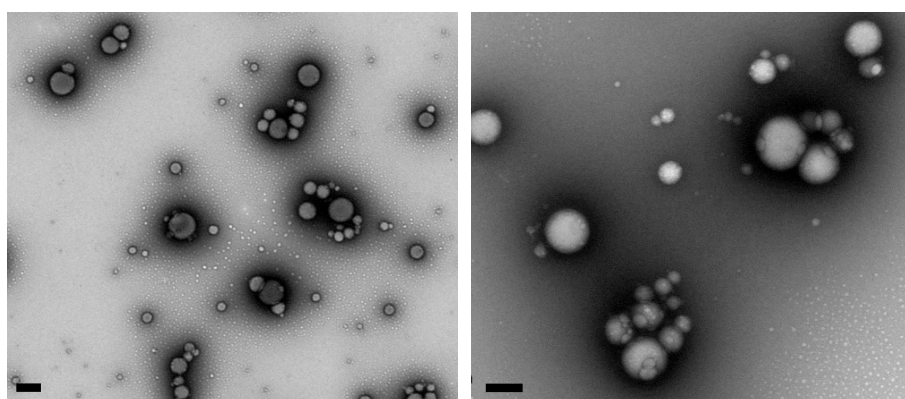

Figure 2: TEM images with negative staining of NC-PA (scale bar = 200 nm).

Stability of the nanoconjugates was evaluated at low (4°C) and physiological conditions (37°C) over a period of 60 days. Interestingly, NC-PA exhibited excellent colloidal stability independently of the storage temperature (**Figure 3**). No aggregation was observed, and the distribution remained narrow over the whole period.
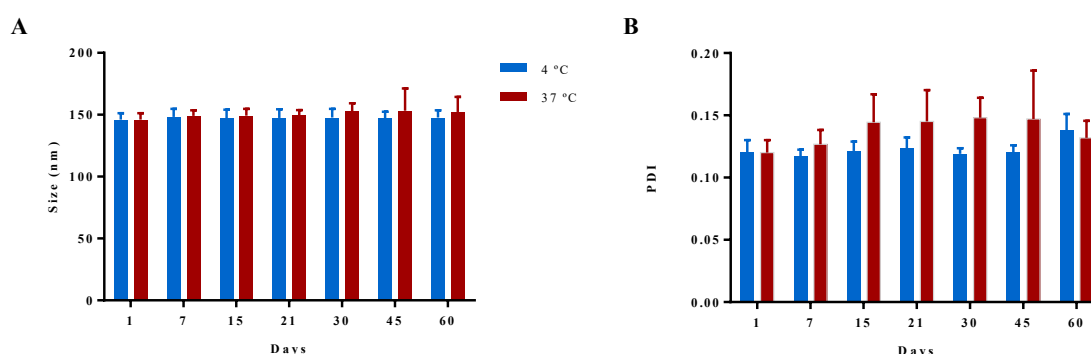

Figure 3: Stability tests performed for NC-PA stored at 4 and 37°C for 60 days, represented in terms of (A) particle size, and (B) PDI. Data represent the mean ± standard deviation (n = 3).

The loading rate of PA is similar to the feed composition determined for PA conjugate since the nanoconjugates are completely formed from the esterified poly(malic acid), no additive has been introduced during the nanoprecipitation step. Therefore, it corresponds to approximately 16 wt% of PA in the final NC-PA. This loading is much higher than the one obtained with a simple physical encapsulation of pyrazinamide, the esterified drug, in PLGA nanoparticles (around 4 wt%).[16]

Release study

Drug release study of the nanoconjugate NC-PA was conducted at 37°C and physiological pH in PBS over a period of 10 days. Free PA was also assessed as control, no drug degradation was observed in this elapsed time. As shown in **Figure 4**, a gradual and complete drug release was achieved in almost 6 days from the nanoconjugate. The initial release of 10% at 15 minutes can be attributed to free PA adsorbed on nanoconjugate surface and not attached to the polymer. As expected with this kind of drug delivery system, a sustained release of PA with no burst release was observed through the hydrolysis of the ester linker between PA and PMA polymer.
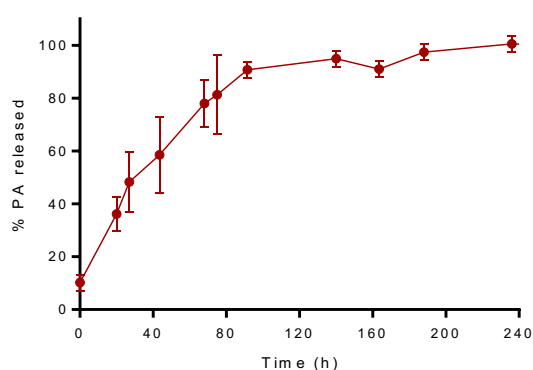

Figure 4: *In vitro drug release of NC-PA in PBS buffer at 37°C. Data represent the mean ± standard deviation (n = 3).*

These drug-controlled release results are desirable in overall TB treatment,[31] once a unique dose is able to maintain therapeutic concentration over a long period and consequently, minimize the drug toxic effects during TB therapy, which may help in increasing patient compliance.

In vitro internalization and cytotoxicity studies

Cytotoxicity of PA nanoconjugates was monitored by MTT assay. NC-PA formulation was incubated with macrophage cells in different ranges of increasing concentrations for 48 hours. Results (**Figure 5)** expressed by means of percentage of cell viability showed that nanoconjugates did not exhibit a toxic potential for the majority of concentrations tested (cell viability over 70%).
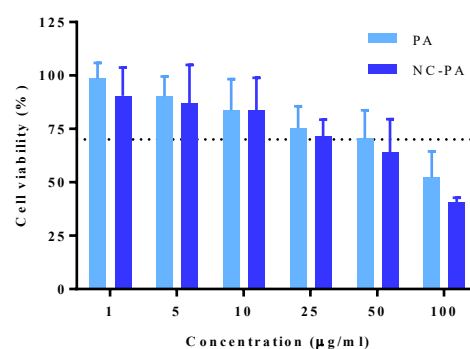

Figure 5: Percentage of cell viability over ranges of nanoconjugates concentrations incubated with RAW 264.7 macrophages for 48 hours. Results express the cytotoxic profiles of PA and NC-PA. Data represent the mean ± standard deviation (n = 3).

Toxicity observed must come exclusively from drugs inherent in the constitution of nanoconjugates since previous studies carried out by our team have shown that PMA has no toxicity to these cells even at concentrations much higher than those used in this work (unpublished work, see **Figure S3,** supporting information). Both free drug and PA nanoconjugates did not present a toxic potential up to 25μg/mL. Above this concentration, cell viability decreased achieving 52 and 40% for free PA and NC-PA, respectively, at 100μg/mL. The higher cell viability observed for free PA could be explained by drug physicochemical properties. As PA is weakly hydrophobic and highly ionized at physiological pH,[9] it is less likely that this molecule will cross the cell membrane, causing a lower cell death than PA nanoconjugates which are internalized by macrophages as showed below. Similar behavior was described by Heifets and co-workers,[32] who reported unexpected higher minimum inhibitory concentration results for PA than for

pyrazinamide against susceptible *M. tuberculosis* strain. The authors associated this finding to inefficient solubilization of PA stock solution into water, which leads to the formation of insoluble precipitates after dilution in the culture medium. Similarly, to this study, the toxic effect of free PA used in this work may be underestimated.

The main triggering factor for tuberculosis management is the administration of anti-tuberculosis drugs in therapeutic quantities at the target sites i.e. alveolar macrophages. These cells are an interesting target in TB treatment, once after inhalation of *M. tuberculosis*, bacteria infect alveolar macrophages and inhibit the phagosome-lysosome fusion, deactivating the defensive mechanisms of these cells and using them as a reservoir to replicate and survive for a long period.[1] Therefore, in order to propose an efficient nanocarrier to fight against TB, it is relevant to assure the capacity of macrophages to uptake nanoparticles. For this reason, PA nanoconjugates developed in this work were fluorescently labeled (NC-PAFLU) and incubated with macrophages at 10 µg/mL (subtoxic concentration) from 0.5 to 6 hours, at 37°C. Internalization of NC-PAFLU by cells was followed by confocal microscopy and results are reported on **Figure 6**. According to the observations, red fluorescence inside cells demonstrated that nanoconjugates were effectively taken up by macrophages over time. Besides, these results pointed out that nanoconjugates were located within the cytoplasm rather than merely attached on the cell membrane. This ability to spread within cell content expressed by NC-PAFLU is particularly interesting in TB therapeutic since nanoconjugates can easily face mycobacteria and release drugs directly on the disease target site.
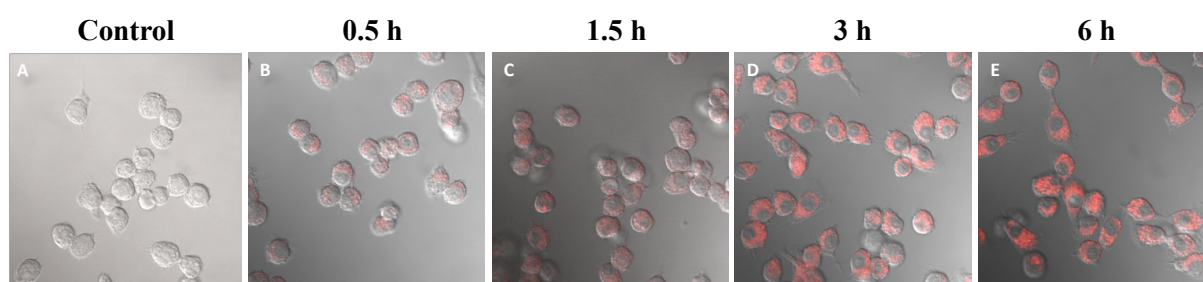
Control	0.5 h	1.5 h	3 h	6 h

Figure 6: Uptake kinetics of NC-PAFLU incubated with RAW 264.7 macrophages cell line at 10 µg/ml for different time intervals. (A) Control (cells without treatment), (B) 0.5 h, (C) 1.5 h, (D) 3 h, (E) 6 h.
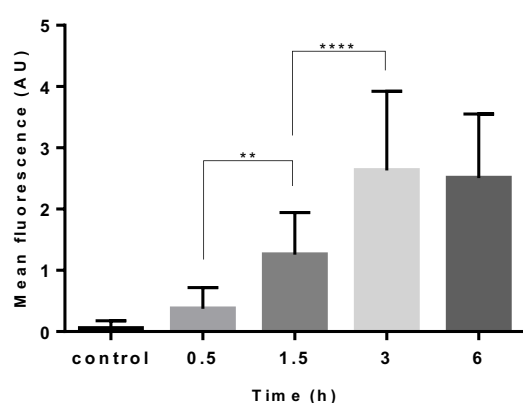

***Figure 7**: Quantification of fluorescence inside cells after incubation with NC-PAFLU at 10 µg/mL over a range of time points. Data represent the mean ± standard deviation. **: $p < 0.05$ and ****: $p < 0.0001$.*

Mean fluorescence inside cells was quantified to investigate the kinetics of the nanoconjugate. Data in **Figure 7** express a general profile for NC-PAFLU with increasing fluorescence over time to a maximum value after 3 hours of incubation. No significant change was observed at 6 hours. At 3 hours, the internalization of nanoconjugates by macrophages was maximal. Finally, NC-PA and PA toxicity were quantitatively expressed by means of IC_{50}. In order to induce 50% cell death, doses of 85.42 and 127.4 µg/mL are required for NC-PA and PA respectively. According to these results, NC-PA is safe, since its IC_{50} is far higher than the concentration necessary for an efficient cell uptake (10 µg/mL). This finding corroborates the main goal of this work in proposing safe nanoconjugates that can effectively be taken up by macrophages and improve TB treatment.

Conclusions and Summary

In this work, we demonstrated that PA biodegradable nanoconjugates were successfully synthesized as a novel and smart strategy for lung administration. Lateral carboxylic groups of PMA were directly conjugated with PA by a simple esterification reaction, ensuring conjugates to self-assemble into nanometric, negatively surface charged and spherical nanoconjugates. NC-PA evidenced a sustained drug release, suggesting the ability of this nanocarrier to maintain drug concentration over time and consequently, to reduce doses and frequency of administration. Allying these findings with the relevant cell culture results, which evidenced that nanoconjugates were effectively taken up by cells for 6 hours and did not present a cytotoxic profile for a wide range of concentrations, we concluded to the discovery of an innovative material with a promising potential in reducing side-effects and improving TB therapy. These preliminary results encourage to move with these nanoconjugates to the perspective of entrapping them into trojan microparticles to enable pulmonary administration and delivery on alveolar macrophages.

Conflict of Interests

The authors declare no conflicts of interest. For signed statements, please contact the journal office: editor@precisionnanomedicine.com

Quote as: Pinto S.C., Moine L, Tessier B, Nicolas V, dos Santos O.D.H., Fattal E., Pyrazinoic acid-Poly(malic acid) biodegradable nanoconjugate for efficient intracellular delivery, Precis. Nanomed. 2019;2(3):303-317, https://doi.org/10.33218/prnano2(3).190523.1

Bibliography

[1]   D. G. Russell, C. E. Barry, and J. L. Flynn, "Tuberculosis: What We Don't Know Can, and Does, Hurt Us," Science (80-.)., vol. 328, no. 5980, pp. 852–856, May 2010.

[2]   World Health Organization, Global tuberculosis report 2017.

[3]   L. C. du Toit, V. Pillay, and M. P. Danckwerts, "Tuberculosis chemotherapy: current drug delivery approaches.," Respir. Res., vol. 7, no. 1, p. 118, Sep. 2006.

[4]   I. P. Kaur and H. Singh, "Nanostructured drug delivery for better management of tuberculosis," J. Control. Release, vol. 184, pp. 36–50, Jun. 2014.

[5]   G. Maartens and R. J. Wilkinson, "Tuberculosis," Lancet, vol. 370, no. 9604, pp. 2030–2043, Dec. 2007.

[6]   Y. Zhang and D. Mitchison, "The curious characteristics of pyrazinamide: a review.," Int. J. Tuberc. Lung Dis., vol. 7, no. 1, pp. 6–21, Jan. 2003.

[7]   D. A. Mitchison and P. B. Fourie, "The near future: Improving the activity of rifamycins and pyrazinamide," Tuberculosis, vol. 90, no. 3, pp. 177–181, May 2010.

[8]   M. H. Cynamon et al., "Pyrazinoic Acid Esters with Broad Spectrum in Vitro Antimycobacterial Activity," J. Med. Chem., vol. 38, no. 20, pp. 3902–3907, Sep. 1995.

[9]   J. P. S. Fernandes, F. R. Pavan, C. Q. F. Leite, and V. M. A. Felli, "Synthesis and evaluation of a pyrazinoic acid prodrug in Mycobacterium tuberculosis," Saudi Pharm. J., vol. 22, no. 4, pp. 376–380, Sep. 2014.

[10]   M. H. Cynamon, S. P. Klemens, T. S. Chou, R. H. Gimi, and J. T. Welch, "Antimycobacterial activity of a series of pyrazinoic acid esters.," J. Med. Chem., vol. 35, no. 7, pp. 1212–5, Apr. 1992.

[11]   M. F. Simões, E. Valente, M. J. R. Gómez, E. Anes, and L. Constantino, "Lipophilic pyrazinoic acid amide and ester prodrugs: Stability, activation and activity against M. tuberculosis," Eur. J. Pharm. Sci., vol. 37, no. 3–4, pp. 257–263, Jun. 2009.

[12]   H. M. Courrier, N. Butz, and T. F. Vandamme, "Pulmonary drug delivery systems: recent developments and prospects.," Crit. Rev. Ther. Drug Carrier Syst., vol. 19, no. 4–5, pp. 425–98, 2002.

[13]   K. Shah, L. W. Chan, and T. W. Wong, "Critical physicochemical and biological attributes of nanoemulsions for pulmonary delivery of rifampicin by nebulization technique in tuberculosis treatment.," Drug Deliv., vol. 24, no. 1, pp. 1631–1647, Nov. 2017.

[14]   D.-D. Pham, E. Fattal, and N. Tsapis, "Pulmonary drug delivery systems for tuberculosis treatment," Int. J. Pharm., vol. 478, no. 2, pp. 517–529, Jan. 2015.

[15]   J. C. Sung et al., "Formulation and Pharmacokinetics of Self-Assembled Rifampicin Nanoparticle Systems for Pulmonary Delivery," Pharm. Res., vol. 26, no. 8, pp. 1847–1855, Aug. 2009.

[16]   D.-D. Pham and N. Tsapis, "Pyrazinamide-loaded poly(lactide-co-glycolide) nanoparticles: Optimization by experimental design," J. Drug Deliv. Sci. Technol., vol. 30, pp. 384–390, Dec. 2015.

[17]   A. L. da Silva, F. F. Cruz, P. R. M. Rocco, and M. M. Morales, "New perspectives in nanotherapeutics for chronic respiratory diseases," Biophys. Rev., vol. 9, no. 5, pp. 793–803, Oct. 2017.

[18]   R. Pandey, A. Zahoor, S. Sharma, and G. . Khuller, "Nanoparticle encapsulated antitubercular drugs as a potential oral drug delivery system against murine tuberculosis," Tuberculosis, vol. 83, no. 6, pp. 373–378, Jan. 2003.

[19]   A. O. Abioye, G. Tangyie Chi, A. T. Kola-Mustapha, K. Ruparelia, K. Beresford, and R. Arroo, "Polymer-Drug Nanoconjugate – An Innovative Nanomedicine: Challenges and Recent Advancements in Rational Formulation Design for Effective Delivery of Poorly Soluble Drugs," Pharm. Nanotechnol., vol. 4, no. 1, pp. 38–79, 2016.

[20]   F. Seidi, R. Jenjob, and D. Crespy, "Designing Smart Polymer Conjugates for Controlled Release of Payloads," Chem. Rev., vol. 118, no. 7, pp. 3965–4036, Apr. 2018.

[21]   P. Loyer and S. Cammas-Marion, "Natural and synthetic poly(malic acid)-based derivates: a family of versatile biopolymers for the design of drug nanocarriers," J. Drug Target., vol. 22, no. 7, pp. 556–575, Aug. 2014.

[22]   J. Y. Ljubimova, M. Fujita, A. V Ljubimov, V. P. Torchilin, K. L. Black, and E. Holler, "Poly(malic acid) nanoconjugates containing various antibodies and oligonucleotides for multitargeting drug delivery," Nanomedicine, vol. 3, no. 2, pp. 247–265, Apr. 2008.

[23]   T. Su et al., "Functionalization of biodegradable hyperbranched poly(α,β-malic acid) as a nanocarrier platform for anticancer drug delivery," RSC Adv., vol. 5, no. 17, pp. 13157–13165, 2015.

[24]   H. Fessi, F. Puisieux, J. P. Devissaguet, N. Ammoury, and S. Benita, "Nanocapsule formation by interfacial polymer deposition following solvent displacement," Int. J. Pharm., vol. 55, no. 1, pp. R1–R4, Oct. 1989.

[25]   T. Mosmann, "Rapid colorimetric assay for cellular growth and survival: Application to proliferation and cytotoxicity assays," J. Immunol. Methods, vol. 65, no. 1–2, pp. 55–63, Dec. 1983.

[26]   N. Grabowski et al., "Surface coating mediates the toxicity of polymeric nanoparticles towards human-like macrophages.," Int. J. Pharm., vol. 482, no. 1–2, pp. 75–83, Mar. 2015.

[27]   B. He, E. Wan, and M. B. Chan-Park, "Synthesis and degradation of biodegradable photo-cross-linked poly(α,β-malic acid)-based hydrogel," Chem. Mater., vol. 18, no. 17, pp. 3946–3955, 2006.

[28]   T. Ouchi and A. Fujino, "Synthesis of poly(α-malic acid) and its hydrolysis behavior in vitro," Die Makromol. Chemie, vol. 190, no. 7, pp. 1523–1530, Jul. 1989.

[29]   T. Kajiyama, H. Kobayashi, T. Taguchi, K. Kataoka, and J. Tanaka, "Improved synthesis with high yield and increased molecular weight of poly(α,β-malic acid) by direct polycondensation," Biomacromolecules, vol. 5, no. 1, pp. 169–174, 2004.

[30] C. J. Martínez Rivas et al., "Nanoprecipitation process: From encapsulation to drug delivery," Int. J. Pharm., vol. 532, no. 1, pp. 66–81, Oct. 2017.

[31] A. Costa et al., "The formulation of nanomedicines for treating tuberculosis," Adv. Drug Deliv. Rev., vol. 102, pp. 102–115, Jul. 2016.

[32] L. B. Heifets, M. A. Flory, and P. J. Lindholm-Levy, "Does pyrazinoic acid as an active moiety of pyrazinamide have specific activity against Mycobacterium tuberculosis?," Antimicrob. Agents Chemother., vol. 33, no. 8, pp. 1252–4, Aug. 1989.
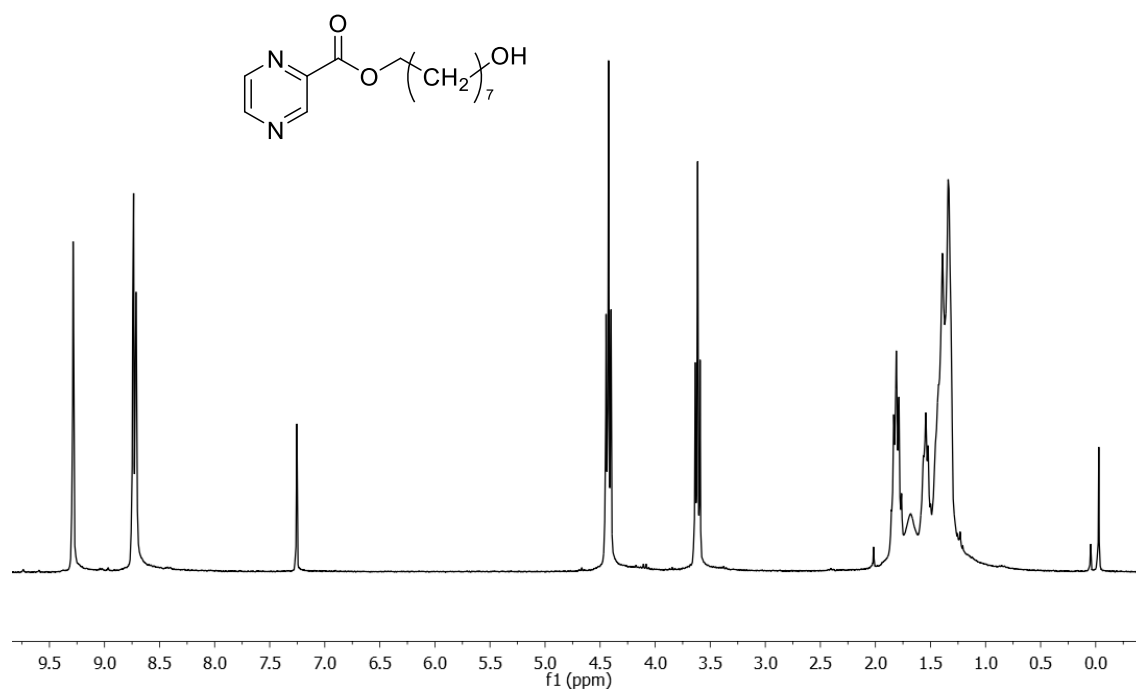
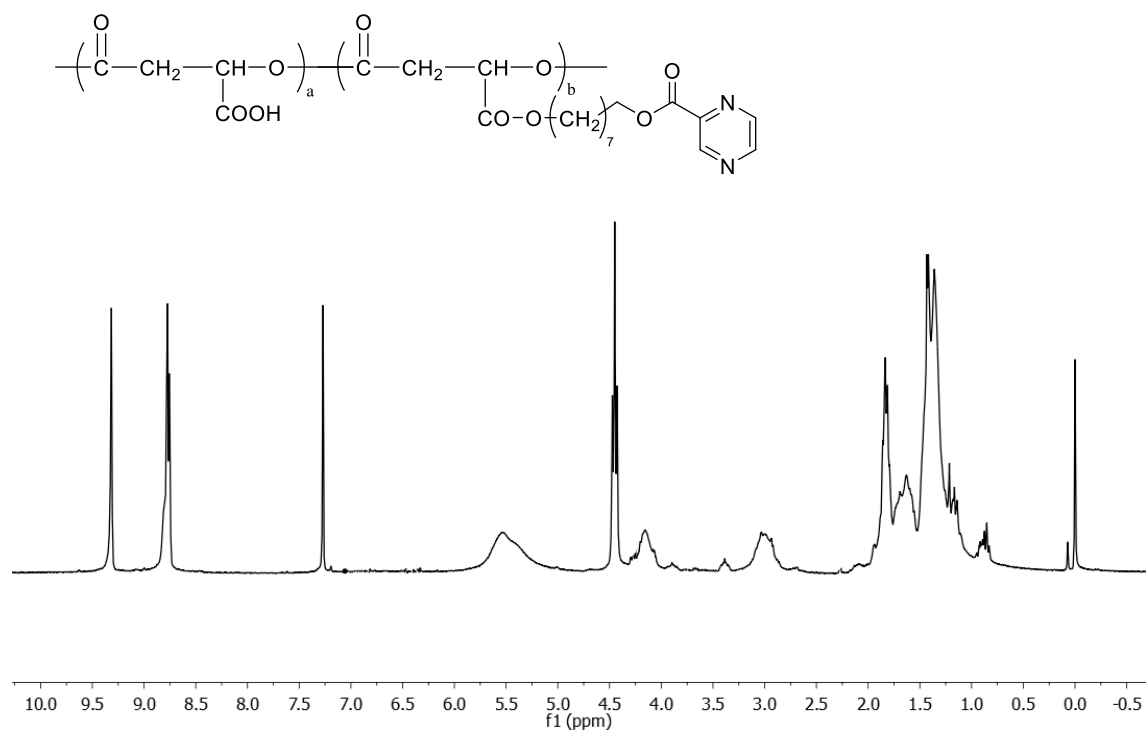**Fig. S1:** *^{1}H NMR spectra of PA:Oct in CDCl$_3$*

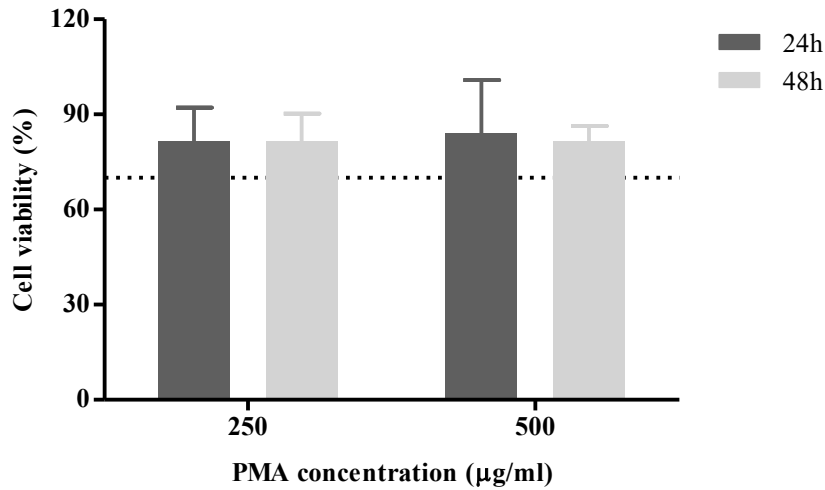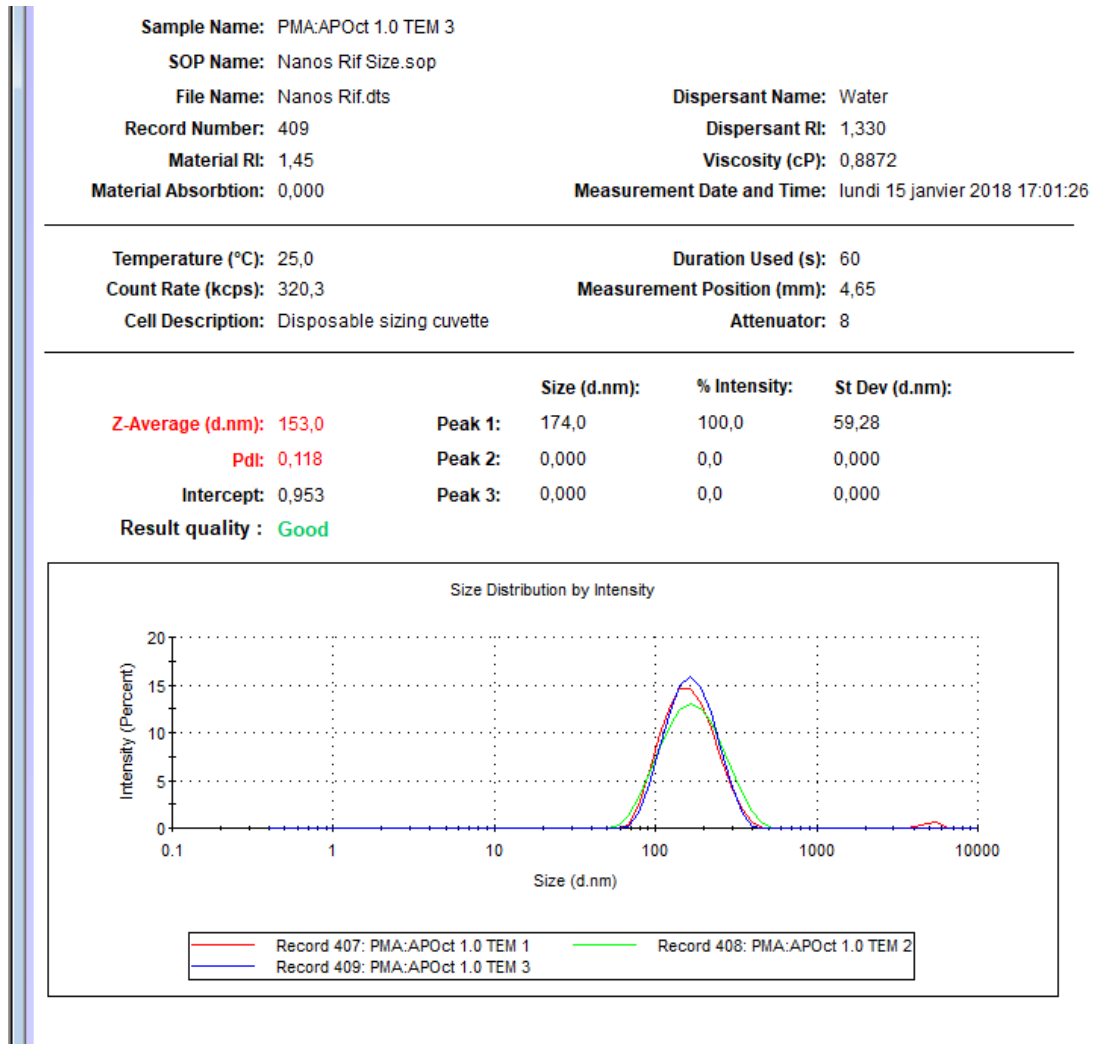**Fig. S2**: *1H NMR spectra of PA conjugate in CDCl3*

Fig. S3: *Percentage of cell viability over poly(malic acid) (PMA) concentrations incubated with RAW 264.7 macrophages for 24h (dark gray) and 48h (light gray). Data represent mean ± standard deviation; n = 3*

Sample Name: NP PMA:APOct 1.0 1ere lot stabilite 1J 1
SOP Name: PMA Bud ZP.sop
File Name: Nanos Rif.dts
Record Number: 378
Date and Time: mercredi 10 janvier 2018 16:31:58

Dispersant Name: NaCl 1mM
Dispersant RI: 1,340
Viscosity (cP): 0,9837
Dispersant Dielectric Constant: 78,5

Temperature (°C): 25,0
Count Rate (kcps): 35,5
Cell Description: Clear disposable zeta cell

Zeta Runs: 17
Measurement Position (mm): 2,00
Attenuator: 9

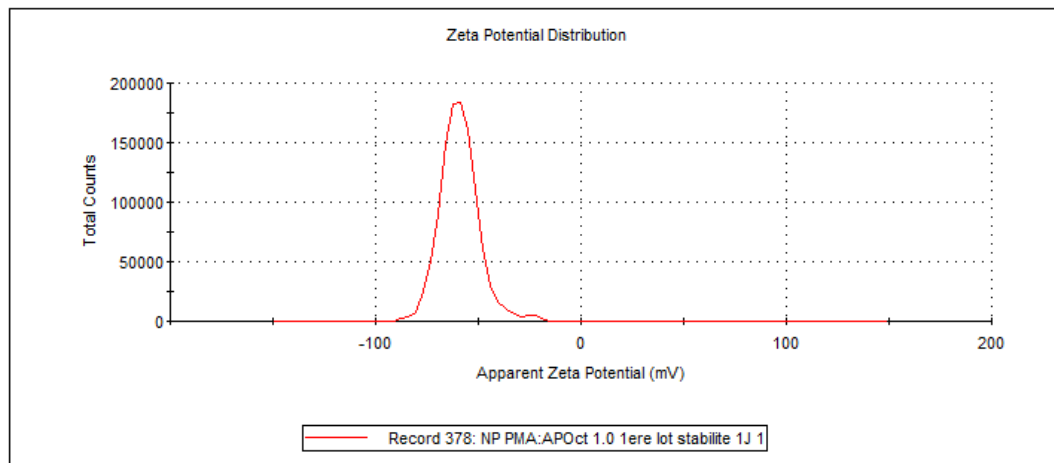|		Mean (mV)	Area (%)	St Dev (mV)
Zeta Potential (mV): -59,0	**Peak 1:**	-59,3	98,6	8,94
Zeta Deviation (mV): 9,62	**Peak 2:**	-24,7	1,4	3,49
Conductivity (mS/cm): 0,133	**Peak 3:**	0,00	0,0	0,00

Result quality : Good

Fig. S4: DLS data of NC-PA